J Solid State Electrochem (2010) 14:1185–1195
DOI 10.1007/s10008-009-0943-x

ORIGINAL PAPER

Characterisation of the aluminium–electropolymerised poly(3,4-ethylenedioxythiophene) system

Fredrik Sundfors · Henrik Gustafsson · Ari Ivaska · Carita Kvarnström

Received: 23 June 2009 / Revised: 11 September 2009 / Accepted: 29 September 2009 / Published online: 14 October 2009

Abstract Poly(3,4-ethylenedioxythiophene) (PEDOT) was electropolymerised on aluminium substrates. The Al/Al oxide/PEDOT junction was studied by electrochemical impedance spectroscopy, comparing the impedance response of the polymer film in oxidised, neutral and reduced form. The p- and n-doping behaviour of the PEDOT films was studied by in situ external reflection Fourier transform infrared spectroscopy during stepwise potential cycling of the films. The Al surface underneath the polymer was analysed with X-ray photoelectron spectroscopy. The impedance spectra indicate that an insulating layer between the metal and the polymer grows thicker during doping of the polymer film. The other techniques used suggest that this interfacial layer consists mainly of Al oxides and fluorides. Neither the conductivity nor the dopability of the polymer is notably affected by the growing of this insulating interfacial layer, which makes the concept of PEDOT electropolymerised on Al promising from an organic electronics applications point of view.

Keywords Poly(3,4-ethylenedioxythiophene) · Aluminium · Electrochemical impedance spectroscopy · In situ external reflection Fourier transform infrared spectroscopy

F. Sundfors · H. Gustafsson · A. Ivaska
Process Chemistry Centre,
c/o Laboratory of Analytical Chemistry, Åbo Akademi University,
Biskopsgatan 8,
20500 Åbo-Turku, Finland

C. Kvarnström (✉)
Department of Chemistry, University of Turku,
Vatselankatu 2,
20014 Turku, Finland
e-mail: carita.kvarnstrom@utu.fi

Introduction

Integration of conducting polymers into electronic devices creates an interface between a metal or semiconductor and the polymer. Electrochemical synthesis of conducting polymers can be performed either on chemically inert electrode substrates such as Pt, Au, graphite, glassy carbon or indium tin oxide (ITO), or on oxidisable metals such as Fe, Al, Zn or Cu.

In future electronic applications, conjugated conducting polymers may play an important role as organic semiconductors. Of special interest are the few polymers that are both p- and n-dopable, since they can transport either holes or electrons, for example in photovoltaic devices. Poly(3,4-ethylenedioxythiophene) (PEDOT) can be both p- and n-doped. The n-doping of PEDOT was first reported in 1994 [1], and a number of publications have since then dealt with the subject [2–7].

Aluminium is highly reactive and has extremely high affinity for oxygen. This leads to spontaneous and instantaneous formation of oxide films, mainly Al_2O_3, upon the exposure of fresh metal surfaces even to traces of air, moisture or both [8, 9]. After electropolymerisation under normal laboratory conditions, oxide will certainly be present in the interface region between the Al substrate and the polymer.

Electrochemical impedance spectroscopy (EIS) is a powerful tool for the analysis of electrochemical processes of metal/polymer systems [10, 11]. With EIS, one can study the properties of the whole system, including the electrode surface, possible oxide layers, the polymer, the electrolyte and even the buried interfaces between these different structures. One single experiment can provide a lot of information about ionic and electronic charge transfer resistances, diffusion coefficients and double-layer and

redox capacitances among others [10, 12–14]. However, the relative contribution from these different processes, from the bulk and the interfaces to the total impedance, can be difficult to separate; therefore, additional information from other techniques is often necessary. In order to understand a system better, one can fit the experimental data to an appropriate equivalent electrical circuit. The model should give a good fit to the experimental data, and most importantly, all the elements should have a clear physical meaning [11, 14]. This can be very difficult if the properties of the system change a lot from one measurement to another, e.g. the polarisation potential of a metal/polymer system is varied in a wide potential range. Then one might need several equivalent electrical circuits in order to describe the response under the varying conditions, or one can simply evaluate the results graphically and risk losing some information.

EIS has been used as a tool for the investigation of Al oxide films and the electrochemical processes taking place at the oxide/electrolyte interface [9, 15–19]. EIS measurements give no information on porous oxide films, since the electrolyte present in the pores short circuits the oxide. An insulating alumina barrier layer situated underneath a porous layer, however, strongly influences the system resistance, and EIS has been used to obtain information about the properties and kinetics of this passivated layer [15–17, 19]. Barrier properties of protective organic coatings on aluminium have also been studied with EIS [12, 20, 21]. A very interesting approach is an integrated setup of in situ attenuated total reflection Fourier transform infrared (ATR–FTIR) spectroscopy and EIS, used for studies of non-conducting organic polymer-coated aluminium surfaces in aqueous solutions [13].

Several EIS studies have been conducted on different PEDOT-based polymers, both in aqueous [22–25] and organic solutions [26–29]. However, the general appearance of the impedance spectra in aqueous and organic solutions is quite similar. To the best of our knowledge, there have not been any reports on EIS studies on electrochemically polymerised PEDOT on aluminium substrates in organic solutions. Bantikassegn et al. studied electrochemically prepared PEDOT with a vacuum-evaporated aluminium contact in a sandwich structure, i.e. Al/PEDOT/ITO [30]. This study showed that PEDOT doped with a small anion, ClO_4^-, did not show any resistive layer due to aluminium oxides, whereas PEDOT doped with a large polymeric anion showed a non-conducting interfacial layer possibly consisting of aluminium oxides. The same group also reported formation of highly resistive interfacial layers between vacuum-evaporated aluminium contacts and polypyrrole (PPy) doped with poly(styrenesulphonate) [31] or tetrafluoroborate (BF_4^-) [32]. The insulating aluminium oxide phase is formed rapidly and is very difficult to avoid when Al/polymer junctions are exposed even to traces of air, because of the high oxygen permeability of many polymers [31].

During the last couple of years, there have been some publications on the subject of conducting polymers on Al or Al oxide. Brânzoi et al. [9] electrodeposited PPy films on pure aluminium and reported the simultaneous formation of non-conducting Al_2O_3 and conducting PPy as a composite material at the electrode surface. Cheung et al. [33] who polymerised pyrrole in propylene carbonate in the presence of tetraethylammonium toluenesulphonate observed the same. Despite a rapid Al_2O_3 layer formation immediately in the beginning of the electropolymerisation, they managed to synthesise PPy on Al. However, the insulating layer acted as a barrier for the electron transfer and largely influenced the polymerisation. Teoh et al. [34] synthesised polyaniline–Al_2O_3 composite nanofibres chemically by seeding with alumina nanofibres. There was strong interaction between the polymer and Al_2O_3, and the conductivity of the composite decreased when the Al_2O_3 content was increased. Beck et al. successfully synthesised PPy on Al substrates in both organic [35] and aqueous solutions [36, 37]. They reported that the pretreatment of the Al substrates naturally played a very important role in the PPy film formation and in the electrochemical properties of the Al/PPy structure and that PPy might become overoxidised due to the high local current densities inside the Al_2O_3 pores. EIS measurements on the Al/PPy films clearly showed a high-frequency semicircle that was strongly influenced by the thickness of the Al_2O_3 interlayer between Al and PPy.

FTIR spectroscopy has been shown to be a useful technique for in situ studies of the doping behaviour of conducting polymer films. Neutral, p-doped and n-doped films all show different FTIR spectra with doping-induced vibration bands arising during oxidation and reduction [3]. Combining FTIR and EIS would provide results giving a deeper understanding of the aluminium/polymer system. The two spectroscopical techniques are complementary: FTIR gathers information close to the polymer surface, while EIS detects changes within the whole system [13].

Ever since the 1970s, X-ray photoelectron spectroscopy (XPS) has been used to study interfaces between polymers and metals [38]. XPS spectra can be of great help in determining various species formed in the interfacial layer during polymerisation on metal or deposition of metal on polymers.

We have previously [6] studied the p- and n-doping of PEDOT electrosynthesised on Al. The doping behaviour of PEDOT on Al was shown to be otherwise similar to the behaviour of PEDOT on chemically inert Pt, but after n-doping of PEDOT on Al, the oxidation current peaks were

shifted towards potentials that were more positive. We suspect this shift to be due to structural changes in the interfacial oxide region between Al and the polymer film.

In this work, we study the Al/Al oxide/PEDOT junction with EIS and XPS and the p- and n-doping of the polymer with FTIR spectroscopy. In order to understand the properties of the Al/PEDOT junction better, the EIS results were compared with the EIS behaviour of bare Al and Pt/PEDOT films in 0.1 M tetrabutylammonium hexafluorophosphate ($TBAPF_6$) in acetonitrile (ACN).

Experimental details

Chemicals

ACN (Riedel-de Haën) was freshly distilled over calcium hydride and purified by drying over superactive alumina (150 mesh, Aldrich) before measurements. Alternatively, ACN (Fluka, puriss, H_2O ≤0.001%), stored over molecular sieve, was used as obtained. $TBAPF_6$ (Fluka) was dried under vacuum before use. The monomer 3,4-ethylenedioxythiophene (EDOT) was used as obtained from Bayer. Great caution was taken in order to protect the electrolyte from atmospheric oxygen and water throughout the experiments. All solutions were deoxygenated with nitrogen before use, the EIS measurements were performed under nitrogen atmosphere saturated with ACN.

Electropolymerisation, doping and electrochemical impedance spectroscopy

A conventional three-electrode one-compartment electrochemical cell was used in all electrochemical experiments. For the XPS measurements, PEDOT(PF_6) was electropolymerised on Al plates with accessible areas ~50 mm^2 (Merck, pro analysis). Otherwise, a teflon-sealed 0.79 mm^2 Al disc (Strem Chemicals, 99.9995%), or alternatively, a glass-sealed 0.79 mm^2 Pt disc was used as the working electrode. A platinum wire was used as the counter electrode, and a silver wire coated with silver chloride was used as the reference electrode. All dc potentials (E_{dc}) are referred to this pseudo reference electrode, calibrated vs the ferrocene (Fc)/ferrocinium (Fc^+) redox couple in 0.1 M $TBAPF_6$–ACN ($E_{1/2}$=0.35 V vs Ag/AgCl). Before each experiment, the working electrode was mechanically polished with 1 μm diamond paste (Struers) and rinsed with, in turn, ultrapure deionised water and acetone. The experiments were performed at room temperature (22±2 °C). All electrochemical experiments were performed using an Autolab general-purpose electrochemical system and Autolab frequency response analyser system (AUT30. FRA2-AUTOLAB, Eco Chemie, B.V., the Netherlands).

PEDOT(PF_6) films were made on Al by first applying a current pulse of 64 mA/cm^2 for 0.1 s and followed by potential scanning between −0.9 and 1.25 V. In the case of Pt, the PEDOT(PF_6) films were made by potential scanning between −0.9 and 1.25 V. The potential scan rate used was 100 mV/s. The monomer solution contained 0.1 M EDOT and 0.1 M $TBAPF_6$ in ACN.

After polymerisation, the PEDOT(PF_6) films were cycled in the potential range from −0.7 to +0.8 V (p-doping) at the scan rate of 50 mV/s in 0.1 M $TBAPF_6$–ACN. The impedance response of the films being stepwise reduced (n-doping) was then measured at four different potentials (E_{dc}) in the following order: 0.6, −0.4, −1.0 and −2.0 V. At these potentials the PEDOT(PF_6) film is in p-doped (0.6 and −0.4 V), neutral (−1.0 V) and n-doped (−2.0 V) form [1, 6]. Both p- and n-doping of PEDOT(PF_6) on Al have been discussed in more detail in Ref. [6]. After this, the polymer films were once again p-doped, followed by n-doping and simultaneous impedance measurement according to the previous step. This procedure was completed three times.

The impedance spectra were recorded in the frequency range 100 kHz to 100 mHz using a sinusoidal excitation signal (single sine) with an excitation amplitude (ΔE_{ac}) of 10 mV. The electrodes were equilibrated for 120 s at each E_{dc} before performing the EIS measurements.

Fourier transform infrared spectroscopy

The in situ external reflection measurements were made in a homemade spectroelectrochemical cell, the setup of which has previously been described by Kvarnström et al. [39]. A Bruker IFS66S spectrometer with an MCT detector was used to record the FTIR spectra. The spectra were recorded at stepwise increasing constant potentials. For each spectrum, 32 interferograms with the resolution of 4 cm^{-1} were coadded. Peaks extending upwards represent species formed in the electrochemical reaction in the film, and peaks extending downwards are from depleted species.

External reflection FTIR spectra were taken in situ during stepwise oxidation and reduction of a freshly prepared PEDOT(PF_6) film on Al in 0.1 M $TBAPF_6$–ACN. The p-doping spectra were gathered at the potentials −0.9, −0.5, −0.1, +0.1, +0.3, +0.5, +0.7 and +0.8 V and back again to −0.9 V using the same potentials. The potential was always kept constant for 90 s while acquiring the spectra. The n-doping spectra were gathered every 0.1 V between −0.9 and −2.3 V (every 0.2 V during the reverse scan) with the same 90-s waiting period. All the spectra are divided by a reference spectrum, chosen at a potential where no Faradaic current is present: for p-doping at −0.9 V and for n-doping at −1.7 V.

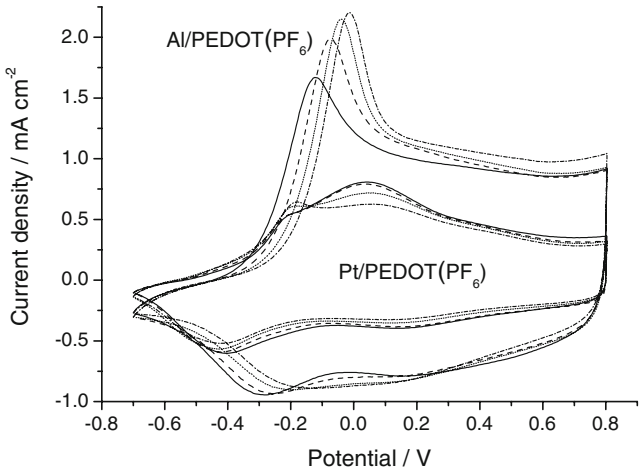

Fig. 1 Cyclic voltammograms of a newly polymerised (*solid lines*) Pt/PEDOT(PF_6) and an Al/PEDOT(PF_6) electrode in 0.1 M $TBAPF_6$–ACN, after the first (*dashed lines*), second (*dotted lines*) and third (*dashed-dotted lines*) EIS measurement cycle (n-doping). Scan rate= 50 mV s^{-1}

X-ray photoelectron spectroscopy

The Al/Al oxide/PEDOT(PF_6) junction was studied by a PHI Quantum 2000 (Physical Electronics, Inc., Eden Prairie, USA) X-ray photoelectron spectrometer. The polymer film, electrosynthesised on an Al plate, was initially covered with epoxy. After curing, the hardened epoxy along with the polymer was mechanically removed from the Al substrate. The elemental distribution of both the epoxy/polymer plug and the metal surface was then analysed. The X-ray source used was monochromatic Al Kα, with the X-ray spot size 100 μm and electron takeoff angle 45°.

Results and discussion

Electrochemical impedance spectroscopy

In order to gain more information about the Al/PEDOT (PF_6) junction, a bare Al electrode and a Pt/PEDOT(PF_6) film electrode were also studied in the same solution, 0.1 M $TBAPF_6$–ACN, using the same measurement conditions and polarisation potentials (E_{dc}). In this way, a better separation was achieved of the contribution from the Al electrode and the polymer film to the impedance response of the Al/PEDOT(PF_6) structure. The Pt/PEDOT(PF_6) and Al/PEDOT(PF_6) films were synthesised under identical conditions, except for the current pulse used to initialise the polymerisation during the synthesis of PEDOT(PF_6) on Al. A more electroactive and probably also thicker conducting polymer film was formed on a well polished Al electrode than on Pt, because of this initial current pulse, as can be seen from the higher current densities for the fresh Al/PEDOT(PF_6) electrode compared with Pt/PEDOT(PF_6) in the cyclic voltammograms in Fig. 1. If the Al electrode was not polished thoroughly before the polymerisation, i.e. it had a thicker oxide layer, we obtained lower currents during the electropolymerisation because of the insulating properties of the Al_2O_3 layer, and consequently a much thinner polymer film was produced.

Pt/PEDOT(PF_6)

Complex plane impedance plots for a Pt/PEDOT(PF_6) electrode at the polarisation potentials (E_{dc}) 0.6, −0.4, −1.0 and −2.0 V in 0.1 M $TBAPF_6$–ACN are shown in Fig. 2. The general appearance of the impedance response resembles those found in the literature for PEDOT in organic solutions [26, 28, 29], and roughly the same changes in the impedance pattern were also observed for Pt/PPy at varying polarisation potentials in $TBABF_4$–ACN [37]. At 0.6 V the impedance response is dominated by an almost vertical capacitive line, but shows a part of a semicircle in the high frequency range, which is possibly merged with a kinetically controlled region to the capacitive line. However, it is quite difficult to graphically interpret this region in detail. In aqueous solutions, this semicircle is not observed, but rather a small 45° Warburg region can be

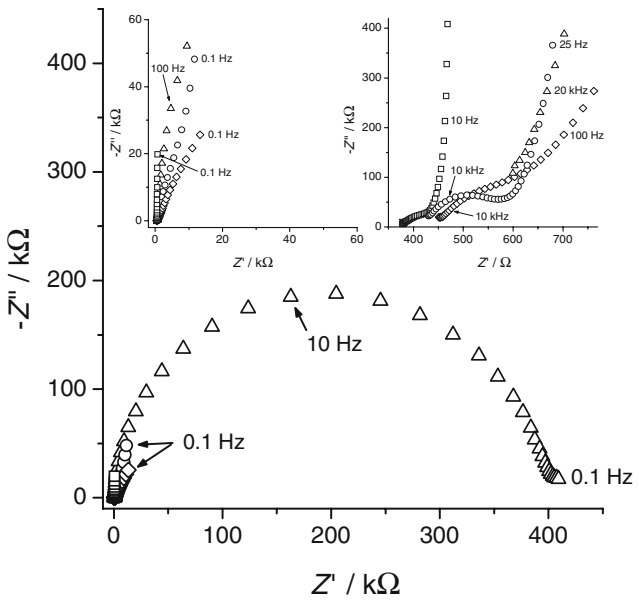

Fig. 2 Complex plane impedance plots during the first measurement cycle of a Pt/PEDOT(PF_6) electrode in 0.1 M $TBAPF_6$–ACN at the polarisation potentials (E_{dc}), 0.6 (*squares*), −0.4 (*circles*), −1.0 (*triangles*) and −2.0 V (*diamonds*). Frequency range=0.1 Hz–100 kHz and E_{ac}=10 mV. The *left inset* shows a rescaled plot for Z' and $-Z''$=0–60 kΩ, while the *right inset* shows a magnification of the high frequency region

found in the high frequency range followed by an almost vertical low frequency region, indicating fast charge transfer kinetics for p-doped PEDOT films [22, 23]. This part of a semicircle at high frequencies was also observed by Carlberg et al. for thin polymer films in 0.1 M $LiClO_4$–ACN [26] and by Eliseeva et al. in 0.1 M $TBAPF_6$ in propylene carbonate, but they could not assign it to any process in the film [29]. However, this semicircle part increased at −0.3 V (vs a saturated silver-chloride electrode) as they stepped the potential in negative direction and reduced the polymer; the same trend can also be seen in our measurements with Pt/PEDOT(PF_6) in 0.1 M $TBAPF_6$–ACN. In our case a fully developed semicircle can be seen at −0.4 V, as shown in the right inset in Fig. 2. This rather small high-frequency semicircle can be due to an interfacial charge transfer process becoming slower with increasing negative potentials, possibly due to an increasing electron transfer resistance at the polymer/electrode interface, as was found by Ren et al. for PPy in aqueous $NaClO_4$ [40].

It is known that PF_6^- can partly decompose into fluorophosphates, fluorides and other mixed derivatives, possibly leading to an accumulation of the decomposition products at the metal/polymer interface, even at Pt [41]. This can be an explanation to the observed charge transfer resistance, i.e. high-frequency semicircle, when using PF_6^- in ACN as the electrolyte. However, it can also be related to the ionic conductivity of the film, because in the case of PEDOT(PF_6) doping anions are expelled from the polymer film as the polymer is being reduced, which can lead to a higher ion transfer resistance. Furthermore, the ionic conductivity of PEDOT in a high concentration electrolyte is mainly dominated by the electrolyte, since the polymer has a very porous structure [22, 23, 26, 28, 29]. This could also be a reason why the semicircle is not observed in aqueous solutions, but only in organic solutions, with obviously a lower polarity and conductivity, affecting the ion transport by the electrolyte in the porous structure. However, if this high-frequency semicircle is due to the organic electrolyte in the polymer pores it would not be expected to show any potential dependence. Therefore, accumulation of decomposition products or higher ion transfer resistance seems more likely. It is, also for us, impossible to assign this semicircle to some specific process in the Pt/PEDOT(PF_6) structure based on these EIS measurements.

At −0.4 V the low-frequency capacitive line also starts to deviate from a vertical line, indicating slower ion transfer inside the polymer film [22]. At the even more negative potential −1.0 V, the impedance plot in Fig. 2 shows a large semicircle in the whole frequency range due to the very high charge transfer resistance of the system because the polymer is an insulator in its neutral state and therefore has a very low electronic conductivity, i.e. high electron transport resistance, of the neutral polymer film [2, 37, 42]. Furthermore, when PEDOT(PF_6) is reduced to its neutral state at −1.0 V, the capacitance of the film drops remarkably to ca. 50 nF from about 80 and 40 μF for 0.6 and −0.4 V, respectively.[1] This is due to the lower amount of electrolyte in the polymer, because when reducing PEDOT doped with the mobile anion PF_6^-, the charge compensating anions together with solvent will be expelled from the polymer [22].

When further reducing the Pt/PEDOT(PF_6) electrode at −2.0 V it will again become more conducting reaching its n-doped state [2]. Now charge compensating cations, TBA^+, and possibly solvent molecules, will enter the polymer film due to electroneutrality reasons [7]. As the charge compensating cations entered the film, the capacitance increased to about 50 μF, comparable to the situation for 0.6 and −0.4 V. However, at −2.0 V a larger deviation from a capacitive line than for the p-doped polymer can be seen in the low frequency range in the left inset in Fig. 2. In the high frequency range shown in the right inset in Fig. 2, a semicircle develops again, but now it merges with a Warburg-type region in the intermediate frequency range. As discussed in the case of −0.4 V, this semicircle can be related to an electron or ion transfer resistance, appearing again as a small high-frequency semicircle as the polymer becomes more conducting in the n-doped state [2]. In the neutral state, at −1.0 V, a big semicircle dominated the whole impedance spectrum because of the high charge transfer resistance of the film. The deviation from the capacitive line at low frequencies and the kinetically controlled intermediate region are probably due to the less mobile negative charge carriers formed during n-doping. It has previously been shown that PEDOT(PF_6) is less conducting in the n-doped state than in the p-doped state [2], and that the level of n-doping is about 1/10 of that of p-doping [7].

Bare Al

Complex plane impedance plots for a bare Al electrode, freshly polished before the first measurement, at the polarisation potentials (E_{dc}) of 0.6, −0.4, −1.0 and −2.0 V in 0.1 M $TBAPF_6$–ACN are shown in Fig. 3. At 0.6 V, a part of a semicircle can be seen, probably due to the formation of a barrier type Al_2O_3 layer on the Al electrode, although the solution was deoxygenated before the measurements, which were performed under nitrogen atmo-

[1] The capacitance was calculated from the relationship $C=1/(2\pi f Z_{im})$ for 0.6, −0.4 and −2.0 V and from $C=1/(2\pi f R)$ for the semicircle at −1.0 V [10].

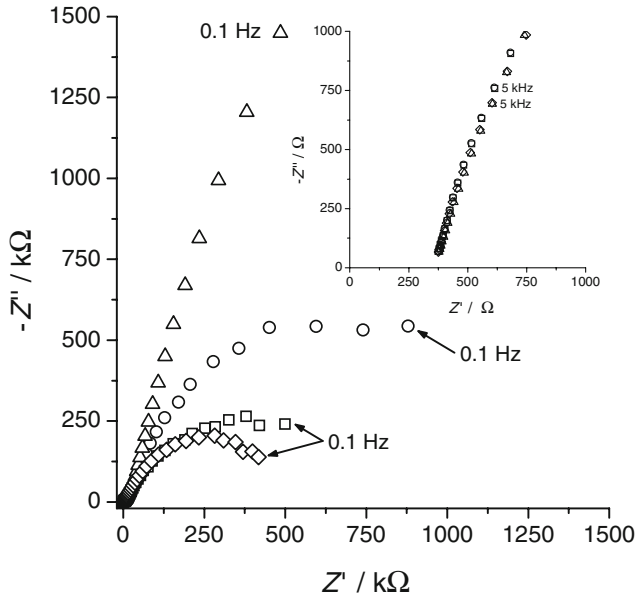

Fig. 3 Complex plane impedance plots during the first measurement cycle of a bare Al electrode in 0.1 M $TBAPF_6$–ACN at the polarisation potentials (E_{dc}), 0.6 (*squares*), −0.4 (*circles*), −1.0 (*triangles*) and −2.0 V (*diamonds*). Frequency range=0.1 Hz–100 kHz and E_{ac}=10 mV. The *inset* shows a magnification of the high frequency region

sphere. The insulating layer is built up when Al is oxidised during the measurement at 0.6 V, since the electrode was freshly polished before measuring. The formation of an insulating layer could also explain the somewhat scattered appearance of the impedance plot: The system is not under steady-state conditions during the EIS measurements, because the thickness of the insulating layer is constantly growing. The resistance of the insulating layer increases as the potential is stepped to −0.4 and −1.0 V, i.e. the diameter of the partly seen semicircle is growing. However, at −2.0 V the resistance drops as part of the aluminium oxide is being reduced and the corrosion products diffuse into the solution, thereby lowering the resistance of the barrier layer. When the EIS measurement cycle is repeated two more times from 0.6 to −2.0 V, without taking the electrode out of the solution in between, the impedance response at 0.6 V is stabilised and a rather constant resistance—now even higher than in the first measurement—is observed (see Fig. 4). The same behaviour was also observed at the other potentials (−0.4, −1.0 and −2.0 V) during the subsequent two measurement cycles (not shown), but in these cases the diameter of the partly seen semicircle also increased slightly between the second and the third EIS measurement cycle. Especially during the third EIS measurement cycle (not shown), it was found that the insulating phase has its lowest resistance at −2.0 V, showing the smallest semicircle at this potential.

Al/PEDOT(PF_6)

The main focus of our study was to find out why the oxidation current peaks are shifted towards more positive potentials after n-doping of Al/PEDOT(PF_6) in 0.1 M $TBAPF_6$–ACN [6], while Pt/PEDOT(PF_6) does not show this behaviour as can be seen in Fig. 1. This shift may be caused by structural changes in the interfacial oxide region between Al and the polymer film. Figure 5 displays the complex plane impedance plots for an Al/PEDOT(PF_6) electrode in 0.1 M $TBAPF_6$–ACN at the polarisation potentials (E_{dc}) 0.6, −0.4, −1.0 and −2.0 V. When generally comparing the impedance response of Al/PEDOT(PF_6) (Fig. 5) to Pt/PEDOT(PF_6) (Fig. 2), we can conclude that additional processes, interfaces or both can be seen in the more complex EIS response of Al/PEDOT(PF_6). When repeating the EIS measurement cycle three times with the Pt/PEDOT(PF_6) system, we can see that the impedance response at 0.6 V is rather constant and no big changes have taken place (see Fig. 6). As shown in Fig. 6, the low frequency response of Al/PEDOT(PF_6) is, however, quite constant for the three repeated measurements, showing a similar vertical capacitive line as for Pt/PEDOT(PF_6). However, in the high frequency region in the inset in Fig. 6 we find some differences between the two electrodes. During the first measurement, Al/PEDOT(PF_6) displays a part of a semicircle, like Pt/PEDOT(PF_6), but additionally

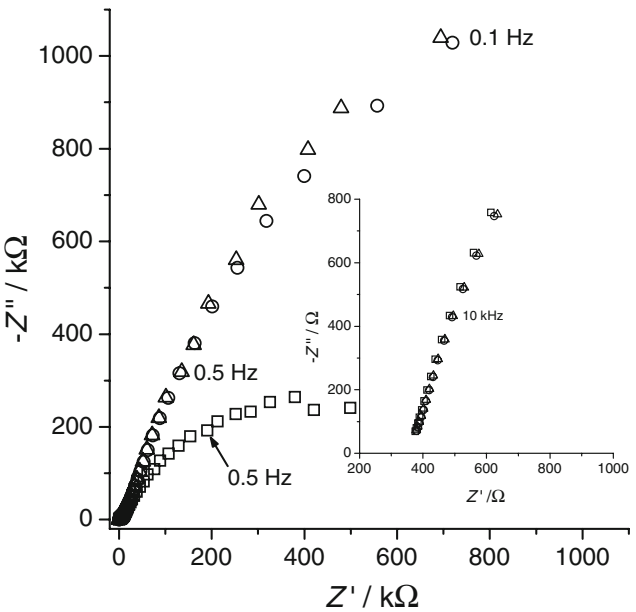

Fig. 4 Complex plane impedance plots of a bare Al electrode at E_{dc}= 0.6 V in 0.1 M $TBAPF_6$–ACN during the first (*squares*), second (*circles*) and third (*triangles*) EIS measurement cycle. Frequency range=0.1 Hz–100 kHz and E_{ac}=10 mV. The *inset* shows a magnification of the high frequency region

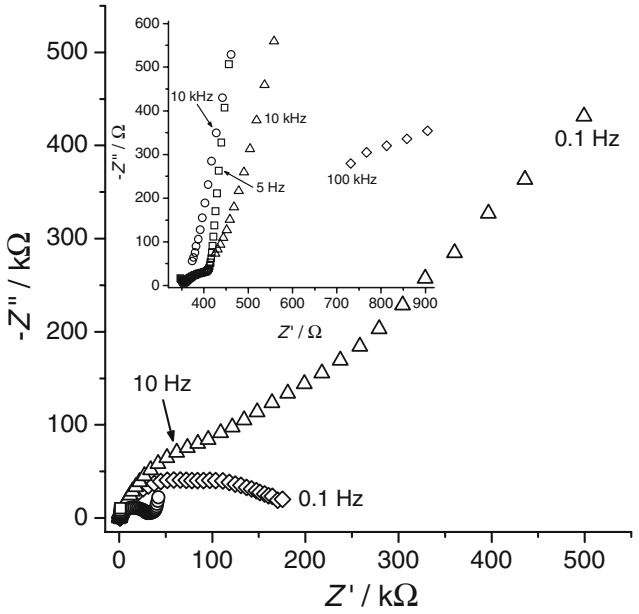

Fig. 5 Complex plane impedance plots during the first measurement cycle of an Al/PEDOT(PF_6) electrode in 0.1 M $TBAPF_6$–ACN at the polarisation potentials (E_{dc}), 0.6 (*squares*), −0.4 (*circles*), −1.0 (*triangles*) and −2.0 V (*diamonds*). Frequency range=0.1 Hz–100 kHz and E_{ac}=10 mV. The *inset* shows a magnification of the high frequency region

a high frequency arch can be seen, which develops into a complete semicircle during the third measurement.

This process is evidently related to the Al/polymer interface, possibly to the growth of a new physical layer of aluminium oxide or an increasing charge transfer resistance, since it is found at very high frequencies and cannot be seen for the Pt/PEDOT(PF_6) electrode. Also Hülser and Beck found a high-frequency semicircle for PPy covered Al, both in organic and aqueous solutions, which they assigned to the PPy/Al_2O_3 interlayer between Al and PPy [36, 37]. Compared to bare Al they found that this semicircle shrank by two or three orders of magnitude for PPy covered Al. Another evidence for the formation of this high-frequency semicircle being related to the Al_2O_3 layer is that a more fully developed semicircle can be seen already during the first EIS measurement for an Al/PEDOT (PF_6) electrode that had only been slightly polished before the synthesis of the polymer film, i.e. it should have a thicker oxide layer (see the inset in Fig. 6). During the electropolymerisation on this "oxidised" Al electrode the currents were much lower and the resultant Al/PEDOT (PF_6) film showed a much lower electroactivity during p-doping in 0.1 M $TBAPF_6$–ACN (not shown), compared to using a more thoroughly polished Al electrode. The part of a semicircle following at slightly lower frequencies is probably related to the PEDOT(PF_6) film or the electrolyte, as previously discussed, since it is constant and has the same magnitude for both Pt/PEDOT(PF_6) and Al/PEDOT (PF_6).

Polarising the Al/PEDOT(PF_6) electrode further in the negative direction to −0.4 V leads to even bigger differences between Al and Pt as electrode substrate (Fig. 7). Already during the first EIS measurement, Al/PEDOT(PF_6) clearly shows a charge transfer resistance at high frequencies, much bigger than that found for Pt/PEDOT(PF_6) (see the inset in Fig. 7). Furthermore, during the second and third EIS measurement cycle at −0.4 V the semicircle clearly increases and is merged with a second semicircle, which is an indication of an additional electrochemical process or a new interface [9].

These semicircles have diameters in the range of tens of kΩ, and one of them is probably related to the formation of insulating Al_2O_3 at the Al/polymer interface. The resistance of this insulating layer is much lower than for bare Al (Fig. 3), as also observed earlier for PPy [36, 37]. Even though the electrolyte solution is deoxygenated before the measurements, only small amounts of oxygen is needed for the formation of an Al_2O_3 layer on a polymer-coated electrode. For Al/PPy, Inganäs et al. found that formation of Al_2O_3 could not be avoided even under vacuum because of

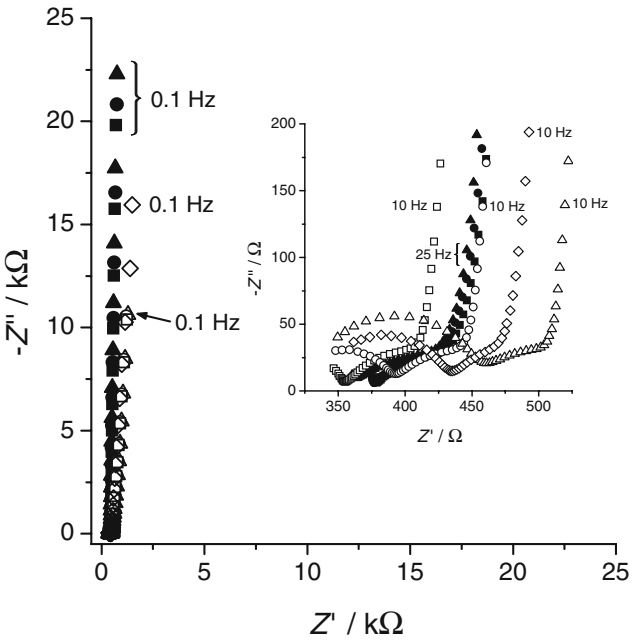

Fig. 6 Complex plane impedance plots of an Al/PEDOT(PF_6) (*open symbols*: *squares*, *circles* and *triangles*) and a Pt/PEDOT(PF_6) (*filled symbols*: *squares*, *circles* and *triangles*) electrode in 0.1 M $TBAPF_6$–ACN at E_{dc}=0.6 V during the first (*open* and *filled squares*), second (*open* and *filled circles*) and third (*open* and *filled triangles*) EIS measurement cycle. Also shown is the impedance response during the first EIS measurement cycle of an Al/PEDOT(PF_6) (*diamonds*) electrode with a thicker oxide layer. Frequency range=0.1 Hz–100 kHz and E_{ac}=10 mV. The *inset* shows a magnification of the high frequency region

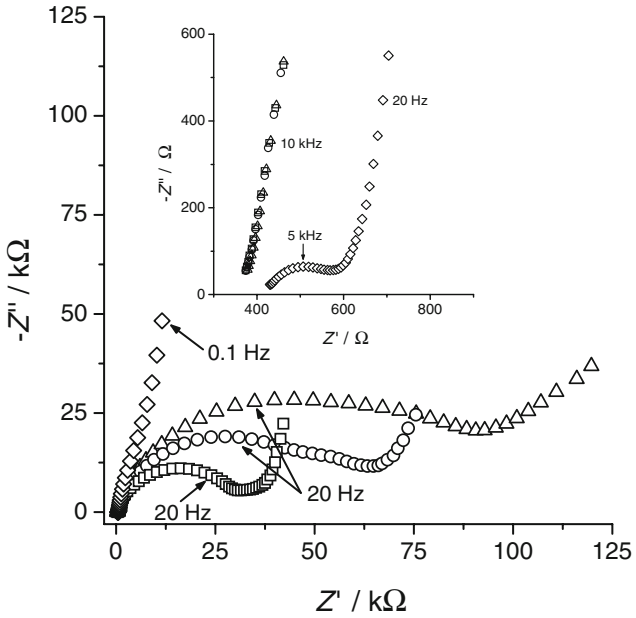

Fig. 7 Complex plane impedance plots of an Al/PEDOT(PF_6) electrode at E_{dc}=−0.4 V in 0.1 M $TBAPF_6$–ACN during the first (*squares*), second (*circles*) and third (*triangles*) EIS measurement cycle and for a Pt/PEDOT(PF_6) (*diamonds*) electrode during the first EIS measurement cycle. Frequency range=0.1 Hz–100 kHz and E_{ac}= 10 mV. The *inset* shows a magnification of the high frequency region

the oxygen absorbed by the polymer when previously exposed to air [32]. The second semicircle may simply be due to an increasing charge transfer resistance between the polymer and the electrode as the insulating phase, most probably consisting of Al_2O_3, is growing thicker. However, it may also be related to decomposition of PF_6^- into a number of products that might react with Al or Al_2O_3 forming various compounds [41], which could explain the growing semicircles as the compounds accumulate at the Al/polymer interface. As for 0.6 V, Pt/PEDOT(PF_6) showed a constant response during the repeated EIS measurements at −0.4 V, which proves that the increasing semicircles are not related to the PEDOT(PF_6) film itself nor to accumulation of products from the decomposition of PF_6^- at the metal/polymer interface. If the latter would be true, we should see a growing semicircle also for the impedance response of Pt/PEDOT(PF_6). The third EIS measurement at −0.4 V in Fig. 7 clearly shows the appearance of a 45° Warburg region at the lowest frequencies.

Comparing the impedance spectrum of Al/PEDOT(PF_6) (Fig. 5) with that of Pt/PEDOT(PF_6) (Fig. 2) at −1.0 V shows some differences. The impedance response of Pt/PEDOT(PF_6) is dominated by a large semicircle in the whole frequency range. We assign this to a high charge transfer resistance of the system due to the insulating properties of the neutral polymer film [2]. The Al/PEDOT (PF_6) electrode displays a semicircle in the high frequency range merged with something that looks like a 45° Warburg region for the low frequencies. One can assume that the first semicircle is related to a charge transfer resistance of the system due to the low electronic conductivity of the polymer film [2], as it roughly has the same magnitude as for Pt/PEDOT(PF_6), and it is fairly constant during the second and third EIS measurement cycles (not shown). Furthermore this semicircle is found exactly in the same frequency region for both Pt/PEDOT(PF_6) and Al/PEDOT (PF_6), with the highest point of the semicircle at f=7.94 Hz in both cases. However, the lower frequency region that looks like a Warburg diffusion region during the first EIS measurement cycle at −1.0 V develops into two semicircles in the second EIS measurements at −1.0 V (not shown): one smaller—though bigger than the constant high-frequency semicircle—and poorly resolved semicircle in the intermediate frequency range and the beginning of a large semicircle for the lowest frequencies. This was even more clearly seen when extending the frequency range for the EIS measurements down to 10 mHz (not shown). The latter semicircle is comparable in size to the impedance response of bare Al at −1.0 V (Fig. 3). We can therefore assign it to the formation of the insulating Al_2O_3 layer. Furthermore, during the third EIS measurement cycle only two semicircles are found: one in the high frequency region and a much larger one partly in the low frequency region.

At the most negative potential, −2.0 V, the interpretation of the impedance spectrum of the Al/PEDOT(PF_6) electrode in Fig. 5 turns more difficult. In the third EIS measurement (not shown), the impedance response developed into two overlapping semicircles with a diameter of about 200 kΩ each. Because these semicircles grow between the three EIS measurement cycles at −2.0 V and because PEDOT should be conducting in the n-doped state, the two semicircles may be assigned to the formation of the Al_2O_3 layer and maybe to the decomposition of the PF_6^- electrolyte, rather than to a charge transfer resistance of the polymer film that should be constant according to the measurements with Pt/PEDOT(PF_6). The largest semicircles during the EIS measurements with Al/PEDOT(PF_6) can again be found at −1.0 V, like for bare Al (Fig. 3), which is probably due to the reduction of Al_2O_3 at this negative polarisation potential, −2.0 V, leading to a thinner barrier layer.

During the EIS measurements of the Pt/PEDOT(PF_6) (right inset in Fig. 2) and Al/PEDOT(PF_6) (inset in Fig. 5), electrodes one can clearly see that the beginning of the impedance response shifts along the Z' axis with more negative polarisation potentials. This has to be related to the PEDOT(PF_6) film, not to the electrolyte, since it was not observed for the bare Al electrode (inset in Fig. 3). In fact, it is an indication that the electronic resistance of the polymer film increases as the film is being reduced [40,

43]. As can be seen in Fig. 2, the Pt/PEDOT(PF_6) electrode has its highest electronic resistance at −1.0 V in the neutral state, while at −2.0 V the resistance is lower because the n-doped film is more conducting [2]. The same phenomenon can be observed for the Al/PEDOT(PF_6) electrode (Fig. 5), except that the response at −2.0 V is shifted towards much higher impedances on the Z' axis. However, this was only observed at the first EIS measurement cycle at −2.0 V. For the following two EIS measurement cycles, the impedance response at −1.0 V was found at the highest impedance along the Z' axis, as for Pt/PEDOT(PF_6). The reason for the response of the first EIS measurement at −2.0 V is unclear.

After synthesis, the fresh PEDOT(PF_6) film was always cycled in the potential range −0.7 to 0.8 V in order to check the electroactivity of the polymer (see Fig. 1). The figure also shows the cyclic voltammograms recorded after each of the three EIS measurement cycles. This was made in order to check if the polymer films showed any degradation due to the EIS measurements, since they are kept for several minutes at quite negative potentials during the EIS measurements. After the third EIS measurement cycle, the Pt/PEDOT(PF_6) electrode had lost about 20% of its electroactivity, whereas the Al/PEDOT(PF_6) electrode showed no degradation at all. The film morphology and Al_2O_3 phase are possibly affected by the consecutive p- and n-doping in the case of Al/PEDOT(PF_6). Cycling of the film may lead to rearrangements in the interfacial Al_2O_3/polymer film region, thereby maximising the electrical and mechanical contact between Al and the polymer film, compensating for the possible electrochemical capacity loss due to film degradation. According to Inganäs et al., irreversible chemical degradation of the PPy surface does not occur when the insulating phase is formed at the Al/polymer interface [32], but the insulating phase is obviously anchored only to Al. However, they studied PPy with vacuum-evaporated Al contacts and did not synthesise the polymer film directly on Al.

Furthermore, the previously observed shift of the p-doping peaks towards more positive potentials after n-doping [6] is again observed in this study for the Al/PEDOT(PF_6) electrode, whereas the peaks for Pt/PEDOT(PF_6) are not shifted after the n-doping (Fig. 1). We suspected this shift to be due to structural changes in the interfacial oxide region between Al and the polymer film. Based on the EIS experiments, one semicircle can be assigned to a growing Al_2O_3 layer at the Al/polymer interface, but it is difficult to assign the other semicircles to any specific process only based on these EIS measurements. In all the EIS experiments with the Al/PEDOT(PF_6) electrode, the diameter of the semicircles increased with the number of the EIS measurement cycles. We must also remember that Al is covered with a polymer film that will affect the properties of the barrier layer, as the soluble species from the dissolution process of Al_2O_3 during the reduction [9] could otherwise migrate more easily into the bulk of the solution.

Fourier transform infrared spectroscopy

The p- and n-doping behaviour of PEDOT(PF_6) on Al was thoroughly studied in situ by FTIR spectroscopy, and the results were compared with those of PEDOT(PF_6) on Pt. During doping, charge carriers are formed in the polymer backbone, and the infrared spectrum becomes dominated by new strong doping-induced infrared active vibration bands, the intensities of which increase continuously with increasing doping level. The vibrations become IR active because of breaking of the bond symmetry, and the vibrations are enhanced because the charge distribution causes changes in dipole moments during vibration [44]. Kvarnström et al. have previously shown by ATR–FTIR spectroscopy that the infrared active vibration bands arising from p- and n-doping of PEDOT(PF_6) films on Pt are nonidentical [3].

The differential spectra (wavenumber region 1,600–700 cm^{-1}) of the p-doping between −0.5 V and +0.8 V are shown in Fig. 8, also showing a spectrum of p-doped PEDOT(PF_6) on Pt. The wavenumbers of the p-doping-induced bands appearing in the case of PEDOT(PF_6) on Al correspond fairly well with those of p-doping of PEDOT(PF_6) on Pt. Differences, however, are seen in the relative intensities of the bands of the PEDOT(PF_6) film at the two metal substrates. These intensity differences indicate variations in the chain length and morphology of

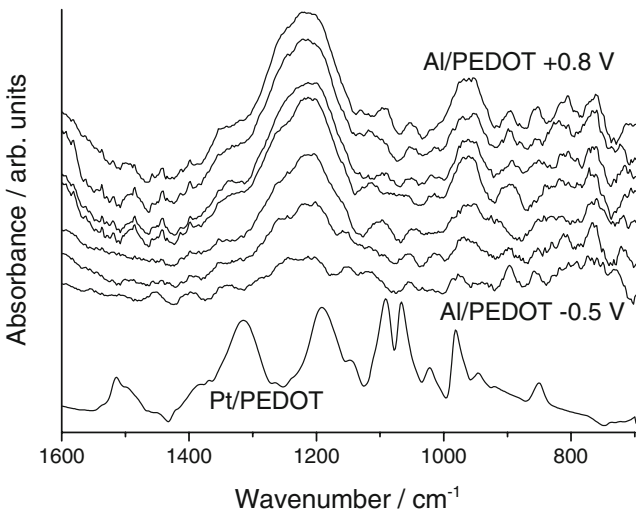

Fig. 8 In situ external reflection FTIR spectra (wavenumber region 1,600–700 cm^{-1}) of PEDOT(PF_6) on Al, being stepwise (−0.5, −0.1, +0.1, +0.3, +0.5, +0.7 and +0.8 V) p-doped in 0.1 M $TBAPF_6$–ACN. Reference spectrum −0.9 V. At *the bottom of the figure* is an ATR–FTIR spectrum of p-doped PEDOT(PF_6) on Pt. The Al/PEDOT(PF_6) spectra have been multiplied by a factor 3 and shifted vertically for the sake of clarity

the polymer depending on the substrate used during electropolymerisation.

The n-doping spectra (wavenumber region 1,600–700 cm^{-1}) between −1.8 V and −2.3 V are shown in Fig. 9, also showing a spectrum of the n-doped PEDOT (PF_6) on Pt. In the latter case, the main n-doping-induced bands appear at 1,280, 1,235, 1,185 (very broad, possibly more than one band), 1,090 and 1,060 cm^{-1}. The corresponding wavenumbers of the bands appearing during n-doping of PEDOT(PF_6) on Al are approximately 1,245–1,250, 1,225, 1,185–1,190, 1,070 and 1,040 cm^{-1}. Furthermore, there are a number of strong bands around the wavenumbers 1,350–1,550 cm^{-1}; these, however, cannot be seen in the Pt/PEDOT(PF_6) spectrum.

The electrochemical conditions during n-doping are quite severe: The potential is kept exceptionally low for a long time. Decomposition of the doping anion PF_6^- is expected to take place at the high negative potentials.

Ferreira et al. [41] studied the partial decomposition of PF_6^- during electropolymerisation of pyrrole in ACN on Fe and Pt electrodes and concluded that a complex mixture of PF_6^-, fluorides, oxyfluorides of phosphorous and metal oxides exists in the interfacial region between metal—both the oxidisable Fe and the noble Pt—and the polymer. The formed oxides and fluorides diffuse through the polymer film: C, N, O, P, F and Fe were found even in the topmost layer of the film. Decomposition of PF_6^- is not a result of the polymerisation processes, since the same decomposition products were detected even when the electrochemical experiments were repeated without pyrrole monomer present in the solution.

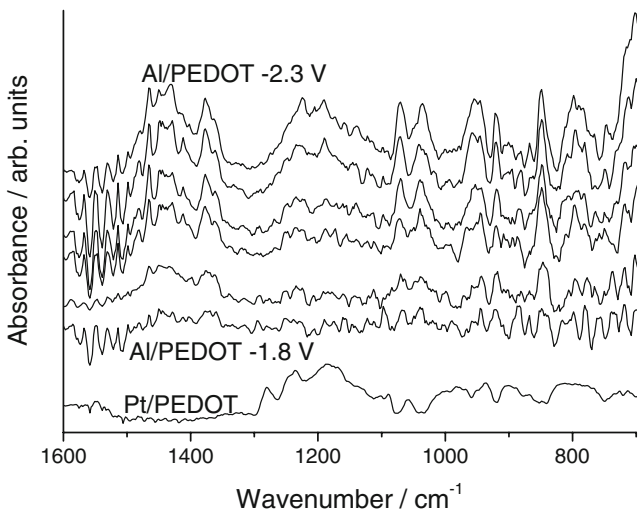

Fig. 9 In situ external reflection FTIR spectra (wavenumber region 1,600–700 cm^{-1}) of PEDOT(PF_6) on Al, being stepwise (−1.8, −1.9, −2.0 V, −2.1, −2.2 and −2.3 V) n-doped in 0.1 M $TBAPF_6$–ACN. Reference spectrum −1.7 V. At *the bottom of the figure* is an external reflection FTIR spectrum of n-doped PEDOT(PF_6) on Pt. The Al/PEDOT(PF_6) spectra have been multiplied by a factor 4 and shifted vertically for the sake of clarity

It seems inevitable that PF_6^- decomposes also in our case. When the Al substrate is exposed to the decomposition products, reactions resulting in aluminium fluorides and similar compounds ought to take place. IR spectra of aluminium fluorides show bands approximately at 965 cm^{-1} (assigned to AlF_3) and 995 cm^{-1} (Al_2F_6) [45], an area where we also see a lot of activity in our spectra. The bands seen around 1,350–1,550 cm^{-1} in the spectra of Al/PEDOT(PF_6) being n-doped (Fig. 9) appear and grow already before the doping-induced bands appear. We cannot definitely assign these bands to any specific species, but they may originate from species formed when the PF_6^- decomposition products react with Al.

The infrared active vibration bands shift to lower wavenumbers with approximately 20 cm^{-1} and thus to lower energies when n-doping PEDOT(PF_6) on Al compared with PEDOT(PF_6) on Pt. It is difficult to give an exhaustive explanation of this. As we have shown earlier [6], no clearly defined Faradaic reduction current peaks are seen in the cyclic voltammograms of PEDOT(PF_6) on Al during n-doping. Since PEDOT(PF_6) might be reduced at different potentials on Pt and Al, there can also be a shift in the wavenumbers corresponding to the n-doping.

X-ray photoelectron spectroscopy

The PEDOT(PF_6) film was mechanically removed from the Al substrate, and the Al surface was then analysed with XPS. The Al 2p XPS spectra of the substrate show the following speciation of aluminium: 11% metallic form, 86% oxidised form and 3% as most probably AlF_3. The fluoride originates from hexafluorophosphate used as the doping anion.

The Al spectral peak corresponding to 3% appears at the binding energy 77.6 eV, whereas AlF_3 reportedly appears at a slightly lower binding energy: 76.3-76.7 eV [46]. As we discussed in the FTIR section, PF_6^- is expected to partially decompose into various species reacting with Al during the electrochemical experiments. The complex mixture resulting from the decomposition gives an explanation why there is a slight shift in the binding energy compared with that of pure AlF_3. XPS reference spectra of Al oxidised in air show no peak at 77.6 eV, otherwise the spectra are identical.

Deposition of Al on conjugated polymers has been shown to affect the polymer chain strongly [47], forming new covalent Al–carbon bonds modifying the geometry of the polymer chain and reducing the π electron conjugation in the polymer backbone. In the case of electrochemically polymerised polythiophene films on Al, covalent bonds between Al and C have been found in the polymer/Al interface but not in the polymer bulk [48, 49].

In our case, electrochemically polymerising PEDOT (PF_6) on Al, no aluminium carbide peaks can be seen in the XPS spectra. If the metal would interact strongly with the polymer chain, Al–C covalent bonds would most probably be formed. We assume that a protective oxide layer is formed on the Al surface before the polymerisation commences, despite polishing the metal surface with diamond paste. Polishing takes place in ambient air, and the oxide layer can freely grow until the Al plate is properly placed in the electrochemical cell containing deoxygenated monomer solution. This oxide layer obviously prevents aluminium to form covalent bonds with the carbon atoms in the polymer chain.

Conclusions

Polymers that are both p- and n-dopable, such as PEDOT, are quite rare and can be considered especially interesting for future electronic devices since these organic semiconductors can transport either holes or electrons. For an organic electronics application, e.g. a photovoltaic device, it is crucial that the charge carriers are able to cross the interface between the polymer and a metal or semiconductor without any problems. This study has concentrated on the structural changes taking place at the Al/Al oxide/PEDOT(PF_6) junction during p- and n-doping of the electrochemically synthesised polymer. No Al–C covalent bonds, which would reduce the π electron conjugation of the polymer chain, are found at the junction. An insulating layer, mainly consisting of aluminium oxides but probably also fluorides, seems to be growing between the metal and the polymer during doping. Interestingly enough, this does not affect the electroactivity of the conducting polymer.

Acknowledgements The grants (06-119, 07-058 and 09-043) provided by the Fortum Foundation to HG are acknowledged. The authors thank Jyrki Juhanoja (Top Analytica Oy Ab) for the XPS analysis. This work is part of the activities of the Åbo Akademi Process Chemistry Centre within the Finnish Centre of Excellence Program (Academy of Finland, 2000–2011). The financial support from the Åbo Akademi Foundation is also acknowledged.

References

1. Pei Q, Zuccarello G, Ahlskog M, Inganäs O (1994) Polym 35:1347
2. Ahonen HJ, Lukkari J, Kankare J (2000) Macromol 33:6787
3. Kvarnström C, Neugebauer H, Ivaska A, Sariciftci NS (2000) J Mol Struct 521:271
4. Alemán C, Curcó D, Casanovas J (2004) Chem Phys Lett 386:408
5. Skompska M, Mieczkowski J, Holze R, Heinze J (2005) J Electroanal Chem 577:9
6. Gustafsson H, Kvarnström C, Ivaska A (2008) Thin Solid Films 517:474
7. Hillman AR, Daisley SJ, Bruckenstein S (2008) Electrochim Acta 53:3763
8. Geetha V, Vaidyan VK (1989) Indian J Pure Appl Phys 27:147
9. Brânzoi V, Pilan L, Golgovici F, Brânzoi F (2006) Mol Cryst Liq Cryst 446:305
10. Musiani MM (1990) Electrochim Acta 35:1665
11. Amirudin A, Thierry D (1995) Prog Org Coat 26:1
12. Hu JM, Zhang JQ, Cao CN (2003) Prog Org Coat 46:273
13. Öhman M, Persson D (2007) Electrochim Acta 52:5159
14. Orazem ME, Tribollet B (2008) Electrochemical impedance spectroscopy. Wiley, New Jersey
15. Bessone J, Mayer C, Jüttner K, Lorenz WJ (1983) Electrochim Acta 28:171
16. Van der Linden B, Terryn H, Vereecken J (1990) J Appl Electrochem 20:798
17. De Laet J, Terryn H, Vereecken J (1996) Electrochim Acta 41:1155
18. Moon S-M, Pyun S-I (1998) J Solid State Electrochem 2:156
19. Sulka GD, Moshchalkov V, Borghs G, Celis J-P (2007) J Appl Electrochem 37:789
20. Bonora PL, Deflorian F, Fedrizzi L (1996) Electrochim Acta 41:1073
21. Hu J-M, Zhang J-T, Zhang J-Q, Cao C-N (2005) Corros Sci 47:2607
22. Bobacka J, Lewenstam A, Ivaska A (2000) J Electroanal Chem 489:17
23. Li G, Pickup PG (2000) Phys Chem Chem Phys 2:1255
24. Sundfors F, Bobacka J, Ivaska A, Lewenstam A (2002) Electrochim Acta 47:2245
25. Lisowska-Oleksiak A, Kupniewska A (2003) Solid State Ionics 157:241
26. Carlberg JC, Inganäs O (1998) J Electrochem Soc 145:3810
27. Lisowska-Oleksiak A, Kazubowska K, Kupniewska A (2001) J Electroanal Chem 501:54
28. Noël V, Randriamahazaka H, Chevrot C (2003) J Electroanal Chem 558:41
29. Eliseeva SN, Spiridonova DV, Tolstopyatova EG, Kondratiev VV (2008) Russ J Electrochem 44:894
30. Bantikassegn W, Inganäs O (1997) Thin Solid Films 293:138
31. Bantikassegn W, Dannetun P, Inganäs O, Salaneck WR (1993) Thin Solid Films 224:232
32. Inganäs O, Lundström I (1984/85) Synth Met 10:5
33. Cheung KM, Bloor D, Stevens GC (1988) Polym 29:1709
34. Teoh GL, Liew KY, Mahmood WAK (2007) Mater Lett 61:4947
35. Beck F, Hülser P (1990) J Electroanal Chem 280:159
36. Hülser P, Beck F (1990) J Appl Electrochem 20:596
37. Beck F, Hülser P, Michaelis R (1992) Bull Electrochem 8:35
38. Burkstrand JM (1979) Phys Rev B 20:4853
39. Kvarnström C, Petr A, Damlin P, Lindfors T, Ivaska A, Dunsch L (2002) J Solid State Electrochem 6:505
40. Ren X, Pickup PG (1997) J Electroanal Chem 420:251
41. Ferreira CA, Aeiyach S, Delamar M, Lacaze PC (1993) Surf and Interface Anal 20:749
42. Gao Z, Kvarnström C, Ivaska A (1994) Electrochim Acta 39:1419
43. Albery WJ, Elliott CM, Mount AR (1990) J Electroanal Chem 288:15
44. Kvarnström C, Ivaska A, Neugebauer H (2001) In: Nalwa HS (ed) Advanced functional molecules and polymers, vol 2. Gordon and Breach Science, Amsterdam
45. Snelson A (1967) J Phys Chem 71:3202
46. Moulder JF, Stickle WF, Sobol PE, Bomben KD (1992) Handbook of X-ray photoelectron spectroscopy. Perkin-Elmer, Eden Prairie
47. Lazzaroni R, Brédas JL, Dannetun P, Fredriksson C, Stafström S, Salaneck WR (1994) Electrochim Acta 39:235
48. Aeiyach S, Bazzaoui EA, Lacaze P-C (1997) J Electroanal Chem 434:153
49. Bazzaoui EA, Aubard J, Elidrissi A, Ramdani A, Lévi G (1998) J Raman Spectrosc 29:799